Current Biology, Volume *23*

Supplemental Information

Selective Chemical Crosslinking Reveals a Cep57-Cep63-Cep152 Centrosomal Complex

Gražvydas Lukinavičius, Darja Lavogina, Meritxell Orpinell, Keitaro Umezawa, Luc Reymond, Nathalie Garin, Pierre Gönczy, and Kai Johnsson

Supplemental Inventory

Supplemental Figures and Tables

Example of localization | **Model** | **List of proteins (Reference)**

A *Proximal end of procentriole*

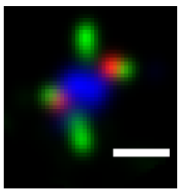

Centrin
SNAP-STIL
C-Nap1

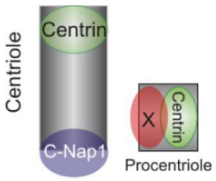

STIL* [1-7]
HsSAS-6* [5, 8]
CPAP C-terminal fragment (967-1338) [5, 9]

B *Proximal end of centriole*

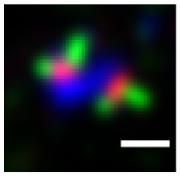

Centrin
SNAP-Cep152
C-Nap1

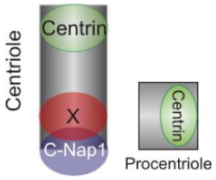

Cep63 (isoforms 1* and 3) [10-12]
Cep57 (isoforms 1 and 3*) [13-15]
Cep70 [16, 17]
Cep152* [5, 18-20]
γ-tubulin [5, 21]
ALMS1 [22]

C *Distal end of centriole*

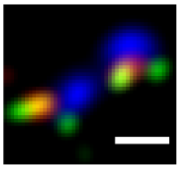

Centrin
SNAP-Cep27
C-Nap1

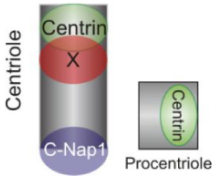

CCCAP [23, 24]
Cep78 [25]
Cep27 [25]
FOP [26, 27]

D *Tips of centriole and procentriole*

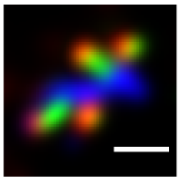

Centrin
SNAP-CP110
C-Nap1

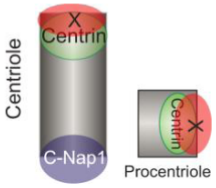

CP110 [5, 28-31]
Cep97* [30]
Centrin2 [21]

E *Unique localization*

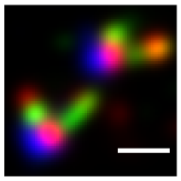

Centrin
SNAP-Cep76 [32]
C-Nap1

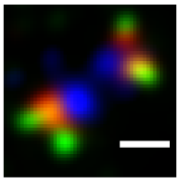

Centrin
SNAP-Centrobin[33,34]
C-Nap1

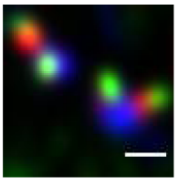

Centrin
SNAP-Cep41 [35]
C-Nap1

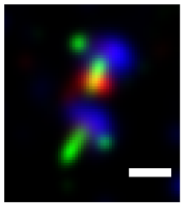

Centrin
SNAP-Cep128 [25]
C-Nap1

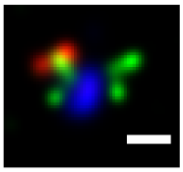

Centrin
SNAP-Cep164 [5, 36]
C-Nap1

F *Structure of centrosome affected by overexpression*

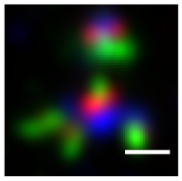

Centrin
SNAP-Plk4* [5, 18, 37, 38]
C-Nap1

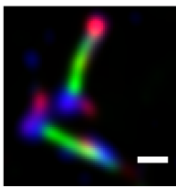

Centrin
SNAP-CPAP full length [39, 40]
C-Nap1

G Fusion proteins not detected on centrosomes:
Cep131** [17], KIAA0841* [25], POC5 fragment (222-304) [41], hSfi1 [42], Cep72** [43], and Cep290 fragment (941-1104) [44]

Figure S1, related to Figures 1 and 3. Centrosomal localization of SNAP-fusions relative to Centrin and C-Nap1. Proteins localized with higher precision in this work than reported in the literature are underlined and italicized. * indicates proteins which were tagged from both C- and N-termini, ** indicates proteins that formed strong cytoplasmic aggregates. Pictures on the left show examples of confocal microscopy image for each category, whereas the corresponding schematic representation is shown on the right. Note that the SNAP-CP110 signal is slightly more distal than the SNAP-Centrin2 signal, as is the case for the corresponding endogenous proteins. The signal of SNAP-Centrin2 was generally less intense on the procentriole, probably due to a less efficient incorporation of the fusion protein compared to the endogenous protein. Expression of SNAP-Plk4 or SNAP-STIL (in case of latter to a smaller extent, hence its placement in panel A rather than F) resulted in multiple procentrioles, while expression of SNAP-CPAP in overly long centrioles (panel F). Of note, cells expressing SNAP-Cep70 occasionally exhibited increased centriole length. The localization of some centrosomal proteins could not be determined very precisely due to a somewhat diffuse signal (γ-tubulin, CCCAP and Centrobin). Cep41 also co-localized with microtubules. SNAP-Sfi1 expressing cells displayed strong reduction in centrosomal centrin signal and the SNAP fusion protein was not localized. Scale bars 500 nm.

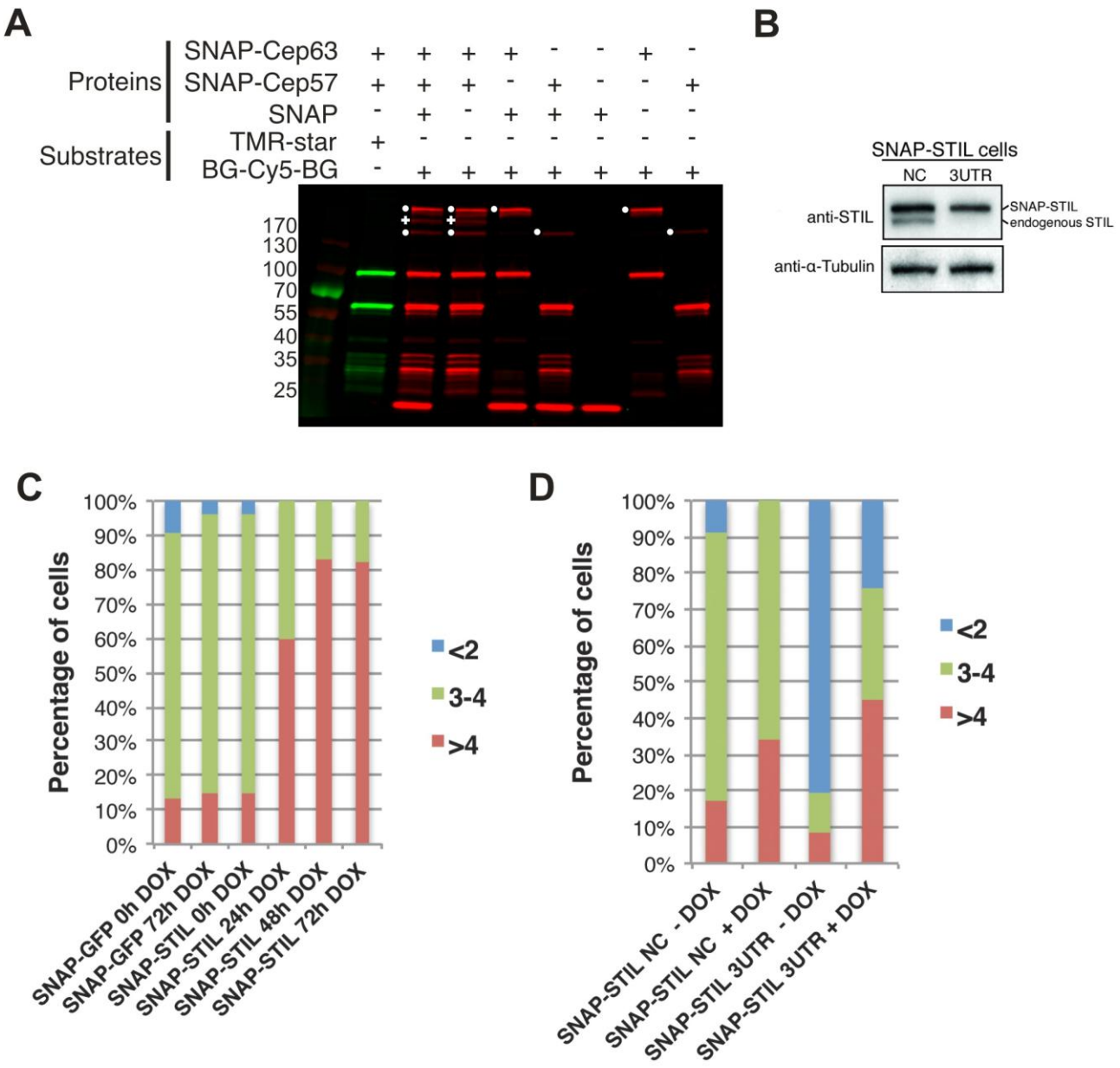

Figure S2, related to Figures 1 and 3. Confirmation of S-CROSS of Cep57 and Cep63. Functionality test of SNAP-STIL. (**A**) In vitro cross-linking of SNAP-Cep57 isoform 3 and SNAP-Cep63 isoform 3. In these experiments, the cross-linker BG-Cy5-BG was utilized that permits the detection of homotypic and heterotypic interactions [45]. Additionally, in some of the experiments SNAP-tag was added as a control. As can be seen from the experiments with isolated SNAP-Cep63 and SNAP-Cep57 (•), both proteins can be cross-linked (in particular SNAP-Cep63), indicating that these proteins form dimers or higher oligomers in solution. In the cross-linking experiment with SNAP-Cep63 and SNAP-Cep57, an additional band indicates a heterotypic interaction (✚). Addition of SNAP-tag does not result in the formation of additional bands, demonstrating the specificity of the cross-

linking. (**B**) Western Blot analysis of cells treated with Stealth RNAi Low GC negative control (NC) or siSTIL-3′UTR (3UTR) and induced concomitantly with doxycycline for 24h. (**C**) Functional analysis of the SNAP-STIL fusion protein. SNAP-STIL expression promotes centriole overduplication. iU2OS:SNAP-GFP and iU2OS:SNAP-STIL cells were induced with doxycyclin at the indicated time points, fixed and stained with antibodies against centrin. Percentage of cells in mitosis with <2, 3-4 or >4 centrioles (based on centrin staining) is shown. (D) SNAP-STIL fusion protein rescues the depletion of endogenous STIL. iU2OS:SNAP-STIL cells transfected with Stealth RNAi Low GC negative control (NC) or siSTIL-3′UTR (3UTR) were left uninduced (-DOX) or induced concomitantly with doxycycline (+DOX), fixed after 72h and stained with antibodies against centrin. Percentage of cells in mitosis displaying <2, 3-4 or >4 centrioles after the indicated treatments is shown. In B and C, each column represents data for ≥50 cells.

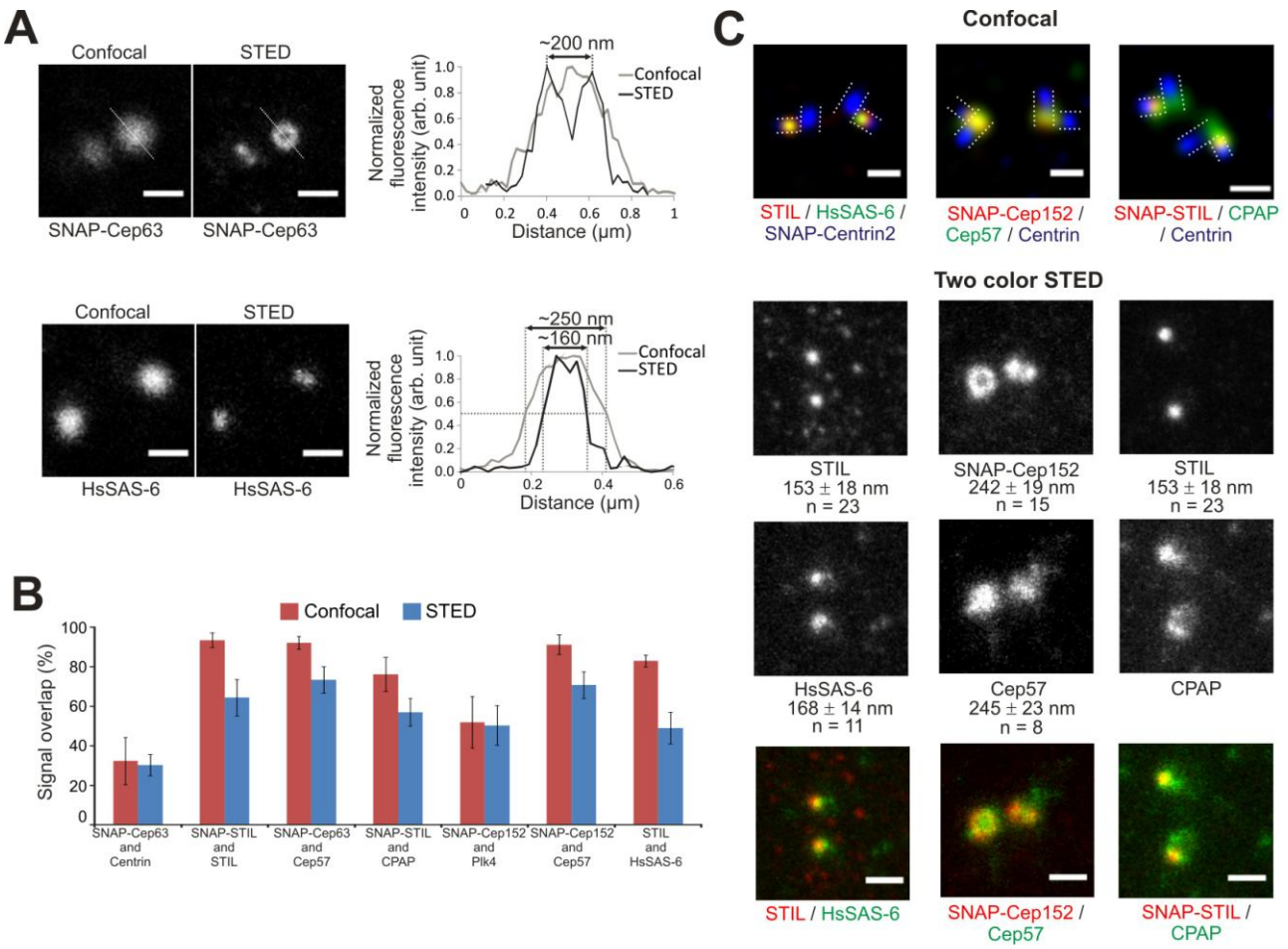

Figure S3, related to Figure 3. Colocalization of centrosomal proteins by confocal and STED microscopy. (**A**) STED imaging of centrosomes. Left: comparison of confocal and STED imaging of SNAP-Cep63 (top) and HsSAS-6 (bottom). Right: corresponding fluorescence intensity profiles. All measurements were performed on proteins of interest stained by Atto647N. Scale bars are 500 nm. (**B**) Estimated fluorescence signal overlap for STED and confocal images presented in **Figure 3** and in this figure. Data are shown as mean ± standard deviation (n > 5). (**C**) Colocalization of STIL, CPAP, HsSAS-6, SNAP-Cep152 and Cep57. Dimensions of structures are given below the STED images. Data are shown as mean ± standard deviation. n - number of centrioles measured. Scale bars are 500 nm.

Table S1, related to Figure 1. Centrosomal proteins expressed as SNAP-tag or CLIP-tag fusion proteins and used for S-CROSS screening.

No.	N-terminal fusion	Length	MW, kDa	Expression level	Centrosomal localization
1	Centrin2	Full	43	++	+
2	POC5	Fragment (222-304)*	34	+/-	-
3	Plk4	Full	133	+	+
4	HsSAS-6	Full	99	+	+
5	α-tubulin	Full	74	++	nd
6	Sfi1	Full	172	+/-	-
7	Cep41	Full	66	++	+
8	STIL	Full (isoform 1)	167	+	+
9	FOP	Full	65	++	+
10	CCCAP	Full	107	++	+
11	γ-tubulin	Full	75	++	+
12	Cep97	Full	121	++	+
13	CP110	Full (isoform 2)	135	+	+
14	Cep290	Fragment (941-1104)*	43	++	-
15	Centrin3	Full	43	++	+
16	Cep27	Full	51	++	+
17	KIAA0841	Full	95	++	-
18	Cep63	Full (isoform 3)	82	++	+
19	Cep76	Full	96	+++	+
20	CPAP	Fragment (967-1338)*	67	++	+
21	Cep57	Full (isoform 3)	55	++	+
22	Cep72	Full	95	++	-
23	Cep70	Full	92	+	+
24	Cep128	Full	74	++	+
25	Cep164	Full	189	++	+
26	Cep152	Full	213	++	+
27	Cep131	Full (3aa deletion at 495-497).	146	++	-
28	Cep78	Full (isoform 2)	104	+	+
29	ALMS1	Full	481	+/-	+
30	CENTROBIN	Full	125	++	+
31	β-tubulin (C-terminal tagging)	Full	74	++	+

*For protein fragments, sequence boundaries are given in parentheses. “+++“ indicates high protein expression level, “++” – medium protein expression level, “+”– low protein expression level and “+/-”– very low protein expression level which is difficult to detect.

Table S2, related to Figure 1. Protein-protein interactions detected via S-CROSS.

No.	Protein pair	S-CROSS score	Reference
1	Cep57 + Cep63	527	New
2	CPAP (967-1338)* + STIL	197	[6, 7]
3	Cep152 + Plk4	120	[18-20]
4	Sfi1 + Centrin 2/3	73 / 42	[42]
5	Cep27 + α-tubulin	20	New
6	β-tubulin + Cep76	9	New
7	Centrin 2/3 + POC5 (222-304)*	5 / 7	[41]
8	KIAA0841 + α-tubulin	5	New
9	γ-tubulin + α-tubulin	4	[46, 47]
10	β-tubulin + Cep57	4	[13]
11	Cep290 (941-1104) + α-tubulin	4	New
12	Cep78 + α-tubulin	3	New
13	β-tubulin + γ-tubulin	3	[46, 47]
14	FOP + POC5 (222-304)*	2	New
15	Cep290 (941-1104)* + Cep41	1	New
16	Centrin 2/3 + C_Cep41	1 / 1	New
17	Cep290 (941-1104)* + Centrin 2	1	New

*For protein fragments, sequence boundaries are given in parentheses.

Table S3, related to Figure 1. Oligomerization detected via S-CROSS.

No.	Protein name	S-CROSS score	Reference
1	CPAP (967-1338)*	276.40	[40]
2	HsSAS-6	175.69	[48]
3	POC5 (222-304)*	128.86	New
4	KIAA0841	127.99	New
5	CP110	117.59	New
6	STIL	46.13	New
7	Cep72	10.95	New
8	Cep78	9.16	New
9	Plk4	8.42	[37]
10	Cep57 (isoform 3)	7.22	[13]
11	CCCAP	5.27	[23]
12	Cep290 (941-1104)*	3.91	[44, 49]
13	γ-tubulin	2.60	[50]
14	Cep76	1.43	New
15	Centrin 3	1.39	[51] by homology with centrin 2
16	Cep97	1.00	New
17	α-tubulin	0.86	[50]
18	FOP	0.29	[27]
19	Cep41	0.15	New
20	Centrin 2	0.01	[51]

*For protein fragments, sequence boundaries are given in parentheses.

Table S4, related to Figure 2. Analysis of overexpression-induced co-localization at centrosomes.

Overexpressed protein	Partner	Exp. No.	N	Correlation with partner protein			Correlation with Centrin		
				R^2	Slope	Significance	R^2	Slope	Significance
SNAP-Cep57	Cep57	I	65	0.61	0.37 ± 0.04	***	0.01	-0.06 ± 0.07	ns
		II	68	0.57	0.41 ± 0.04	***	0.04	0.08 ± 0.05	ns
		III	111	0.65	0.39 ± 0.03	***	0.02	0.10 ± 0.07	ns
	Cep63	I	82	0.33	0.85 ± 0.14	***	0.00	-0.04 ± 0.12	ns
		II	100	0.22	0.33 ± 0.06	***	0.02	0.06 ± 0.05	ns
		III	91	0.11	0.33 ± 0.10	**	0.00	0.05 ± 0.09	ns
	Cep152	I	75	0.17	0.38 ± 0.10	***	0.00	-0.02 ± 0.06	ns
		II	99	0.12	0.33 ± 0.09	***	0.01	0.06 ± 0.05	ns
	γ-tubulin	I	65	0.19	0.18 ± 0.05	***	0.00	0.04 ± 0.09	ns
		II	94	0.14	0.14 ± 0.04	***	0.00	0.01 ± 0.06	ns
	FOP	I	68	0.02	0.02 ± 0.02	ns	0.02	-0.08 ± 0.08	ns
		II	132	0.00	0.01 ± 0.01	ns	0.00	-0.00 ± 0.10	ns
SNAP-Cep63	Cep57	I	44	0.21	0.33 ± 0.10	**	0.14	0.33 ± 0.13	*
		II	44	0.33	0.14 ± 0.03	***	0.02	-0.10 ± 0.11	ns
		III	49	0.19	0.23 ± 0.07	**	0.06	0.12 ± 0.07	ns
	Cep63	I	48	0.83	1.49 ± 0.10	***	0.04	0.16 ± 0.12	ns
		II	65	0.67	1.02 ± 0.09	***	0.02	0.11 ± 0.10	ns
		III	83	0.72	1.16 ± 0.08	***	0.03	0.13 ± 0.09	ns
	Cep152	I	74	0.38	0.81 ± 0.12	****	0.03	0.10 ± 0.08	ns
		II	67	0.51	0.90 ± 0.11	***	0.00	0.04 ± 0.07	ns
		III	96	0.67	1.19 ± 0.09	***	0.09	0.25 ± 0.08	**
	γ-tubulin	I	72	0.24	0.33 ± 0.07	***	0.00	-0.03 ± 0.10	ns
		II	76	0.29	0.31 ± 0.06	***	0.17	0.35 ± 0.09	***
	FOP	I	72	0.02	0.04 ± 0.03	ns	0.03	-0.16 ± 0.11	ns
		II	69	0.03	0.03 ± 0.02	ns	0.00	0.01 ± 0.08	ns
SNAP-Cep152	Cep57	I	65	0.11	0.23 ± 0.08	**	0.03	0.24 ± 0.18	ns
		II	85	0.04	0.09 ± 0.05	ns	0.00	-0.01 ± 0.11	ns
		III	134	0.13	0.14 ± 0.03	***	0.01	0.09 ± 0.09	ns
	Cep63	I	157	0.17	0.45 ± 0.08	***	0.04	0.24 ± 0.10	*
		II	99	0.26	0.79 ± 0.14	***	0.00	-0.09 ± 0.14	ns
		III	107	0.20	0.49 ± 0.08	****	0.01	-0.10 ± 0.09	ns
	Cep152	I	127	0.51	2.44 ± 0.21	****	0.00	0.05 ± 0.20	ns
		II	144	0.62	1.46 ± 0.10	***	0.00	0.00 ± 0.06	ns
		III	124	0.48	1.58 ± 0.14	***	0.05	0.40 ± 0.16	*
	γ-tubulin	I	105	0.11	0.25 ± 0.07	***	0.00	-0.07 ± 0.14	ns
		II	95	0.27	0.24 ± 0.04	***	0.00	-0.00 ± 0.07	ns
	FOP	I	126	0.13	0.12 ± 0.03	***	0.01	-0.08 ± 0.10	ns
		II	103	0.08	0.07 ± 0.02	**	0.01	0.15 ± 0.12	ns

Significance of correlation (Pearson test): **** - ($P < 0.0001$) ultra significant, *** - ($P < 0.001$) extremely significant, ** - ($0.001 < P < 0.01$) very significant, * - ($0.01 < P < 0.05$) significant, ns - ($P > 0.05$) not significant.

Table S5, related to Figure 2. Analysis of siRNA experiments.

Protein	siRNA	Exp. No.	N	Normalized median	25% Percentile	75% Percentile	Significance of difference
Cep57	Control siRNA	I	140	1.00	0.68	1.53	N/A
		II	784	1.00	0.65	1.50	N/A
		III	125	1.00	0.68	1.45	N/A
	Control siLNA	I	323	1.00	0.51	1.55	N/A
		II	1003	1.00	0.61	1.49	N/A
		III	303	1.00	0.55	1.53	N/A
	Cep57 siRNA A	I	111	0.14	0.10	0.25	***
		II	697	0.40	0.22	0.75	****
		III	334	0.11	0.07	0.18	****
	Cep57 siRNA B #	I	39	0.18	0.10	0.43	***
		II	24	0.24	0.13	0.36	***
	Cep63 siRNA A	I	128	0.45	0.29	0.85	***
		II	489	0.61	0.35	1.07	****
		III	224	0.38	0.19	0.62	****
	Cep63 siLNA B	I	111	0.19	0.11	0.33	***
		II	136	0.47	0.22	0.83	****
	Cep152 siLNA A	I	52	0.37	0.22	0.69	***
		II	303	0.64	0.36	1.05	****
	Cep152 siLNA B	I	613	0.67	0.37	1.23	****
		II	234	0.68	0.33	1.24	****
		III	131	0.48	0.27	0.87	****
Cep63	Control siRNA	I	133	1.00	0.66	1.42	N/A
		II	718	1.00	0.67	1.38	N/A
		III	200	1.00	0.74	1.31	N/A
	Control siLNA	I	231	1.00	0.67	1.35	N/A
		II	710	1.00	0.67	1.41	N/A
		III	221	1.00	0.65	1.38	N/A
	Cep57 siRNA A	I	387	0.49	0.31	0.79	***
		II	588	0.56	0.33	0.87	****
		III	285	0.57	0.37	0.77	****
	Cep57 siRNA B #	I	37	0.85	0.52	1.45	ns
		II	67	0.55	0.26	0.89	***
	Cep63 siRNA A	I	106	0.11	0.07	0.23	***
		II	509	0.38	0.20	0.75	****
		III	313	0.26	0.11	0.56	****
	Cep63 siLNA B	I	52	0.12	0.07	0.23	***
		II	552	0.34	0.14	1.05	****
		III	159	0.14	0.07	0.36	****
	Cep152 siLNA A	I	44	0.09	0.06	0.15	***
		II	371	0.42	0.21	0.94	****
		III	119	0.17	0.08	0.32	****
	Cep152 siLNA B	I	509	0.47	0.23	1.19	****
		II	165	0.37	0.17	0.62	****
		III	113	0.30	0.16	0.52	****
Cep152	Control siRNA	I	149	1.00	0.73	1.33	N/A
		II	659	1.00	0.66	1.35	N/A
		III	198	1.00	0.67	1.28	N/A
	Control siLNA	I	178	1.00	0.62	1.40	N/A
		II	795	1.00	0.64	1.35	N/A
		III	269	1.00	0.69	1.29	N/A
	Cep57 siRNA A	I	123	0.44	0.25	0.76	***
		II	562	0.66	0.42	0.94	***
		III	241	0.68	0.44	0.99	****
	Cep57 siRNA B #	I	31	0.43	0.18	0.63	***
		II	67	0.33	0.20	0.52	***
	Cep63 siRNA A	I	67	0.47	0.20	0.72	***
		II	530	0.63	0.37	0.98	***
		III	303	0.50	0.31	0.80	****
	Cep63 siLNA B	I	68	0.08	0.06	0.26	***
		II	327	0.30	0.15	0.64	***
		III	130	0.27	0.15	0.59	****
	Cep152 siLNA A	I	55	0.03	0.02	0.06	***
		II	360	0.17	0.06	0.68	***
		III	134	0.16	0.08	0.67	****
	Cep152 siLNA B	I	404	0.17	0.07	0.40	***
		II	165	0.10	0.05	0.19	****
		III	176	0.13	0.07	0.30	****

Significance of difference between medians of control and gene-targeting siRNA (Mann-Whitney test): **** - ($P < 0.0001$) ultra significant, *** - ($P < 0.001$) extremely significant, ** - ($0.001 < P < 0.01$) very significant, * - ($0.01 < P < 0.05$) significant, ns - ($P > 0.05$) not significant. N is the number of analyzed centrosomes. # - Cells treated with siRNA for 48h.

Table S5, related to Figure 2. Analysis of siRNA experiments. *(continued)*

Protein	siRNA	Exp. No.	N	Normalized median	25% Percentile	75% Percentile	Significance of difference
γ-tubulin	Control siRNA	I	85	1.00	0.75	1.22	N/A
		II	609	1.00	0.75	1.32	N/A
		III	246	1.00	0.81	1.28	N/A
	Control siLNA	I	266	1.00	0.72	1.31	N/A
		II	636	1.00	0.73	1.23	N/A
		III	285	1.00	0.77	1.25	N/A
	Cep57 siRNA A	I	79	0.89	0.56	1.23	ns
		II	538	1.15	0.81	1.44	****
		III	498	0.75	0.59	0.92	****
	Cep57 siRNA B #	I	48	0.31	0.13	0.59	***
		II	93	0.57	0.41	0.82	***
	Cep63 siRNA A	I	110	1.11	0.70	1.51	ns
		II	582	1.09	0.73	1.39	ns
		III	376	0.80	0.66	1.02	****
	Cep63 siLNA B	I	78	1.03	0.74	1.37	ns
		II	496	0.97	0.77	1.20	ns
		III	110	0.87	0.66	1.12	**
	Cep152 siLNA A	I	60	0.84	0.62	1.32	ns
		II	489	0.86	0.63	1.11	****
		III	238	0.80	0.61	1.04	****
	Cep152 siLNA B	I	547	0.99	0.71	1.26	ns
		II	162	0.79	0.59	1.00	****
		III	234	0.66	0.52	0.84	****
Centrin	Control siRNA	I	86	1.00	0.54	1.59	N/A
		II	608	1.00	0.61	1.47	N/A
		III	246	1.00	0.71	1.50	N/A
	Control siLNA	I	266	1.00	0.71	1.59	N/A
		II	635	1.00	0.69	1.55	N/A
		III	285	1.00	0.67	1.38	N/A
	Cep57 siRNA A	I	80	0.64	0.37	0.98	***
		II	537	0.89	0.59	1.29	**
		III	498	0.82	0.51	1.32	****
	Cep57 siRNA B #	I	48	1.18	0.82	1.75	ns
		II	93	0.68	0.39	1.00	***
	Cep63 siRNA A	I	109	1.15	0.71	1.83	ns
		II	581	0.94	0.61	1.39	ns
		III	376	0.89	0.59	1.31	**
	Cep63 siLNA B	I	78	1.31	0.79	1.86	*
		II	495	0.92	0.55	1.29	***
		III	110	0.93	0.61	1.30	ns
	Cep152 siLNA A	I	60	0.78	0.49	1.33	**
		II	488	0.85	0.50	1.26	***
		III	238	0.53	0.30	0.90	****
	Cep152 siLNA B	I	546	1.08	0.73	1.53	ns
		II	162	0.93	0.58	1.38	ns
		III	234	0.82	0.59	1.10	***

Significance of difference between medians of control and gene-targeting siRNA (Mann-Whitney test): **** - ($P < 0.0001$) ultra significant, *** - ($P < 0.001$) extremely significant, ** - ($0.001 < P < 0.01$) very significant, * - ($0.01 < P < 0.05$) significant, ns - ($P > 0.05$) not significant. N is the number of analyzed centrosomes. # - Cells treated with siRNA for 48h.

Supplemental Experimental Procedures

Plasmid construction

pEBTet SNAP_GW, pEBTet GW_SNAP and pEBTetBl_CLIP_GW plasmids were constructed from pEBTet GFP_GW, pEBTet GW and pEBTetBlast, respectively. pEBTet plasmids were characterized previously [52]. Plasmids contain cytomegalovirus-type 2 tetracycline operator (tetO2)-tetO2 promoter which is “switched on” by addition of doxycycline. For N-terminal fusions, SNAP/CLIP genes were amplified by two consecutive PCR’s (introducing FLAG- and His-tags at the N-terminus of SNAP/CLIP-tag), digested with HindIII and KpnI and ligated into the appropriate vector. C-terminal fusions were cloned in an analogous manner by two consecutive PCR’s (introducing FLAG- and His-tags at the C-terminus of SNAP-tag) via NheI and AscI sites. Commercially available entry clones were purchased from Invitrogen or Genecopoeia. All ORFs had stop codon at the end of the gene and were suitable for construction of the N-terminal fusions. pENTR_Age_HsSAS-6 was a kind gift from Petr Strnad. Cep97, CP110, POC5 fragment, Centrin 2 and 3, Plk4, STIL, KIAA0841 and Chr14ORF145 were cloned into intermediate pDONR211 vector by PCR and BP recombination. Sequences were verified by sequencing. The ALMS1 gene was a kind gift from Prof. David Wilson [53] and inserted into pDONR211 vector by adapter ligation and BP recombination.

Cell Culture and Transfection

U2OS cells were obtained from the EACC. U2OS cells were cultured in high-glucose DMEM with GlutaMAX-1 (Invitrogen, Carlsbad, CA) supplemented with 10% fetal calf serum (FCS) in a humidified 5% CO_2 incubator at 37°C. Cells were split every 3-4 days or at confluence. To generate inducible cell lines, cells were transiently transfected with pEBTet expression vector [52] at 80-90% confluence. 48 h after transfection, cells were exposed to the selective medium containing 1 µg/ml puromycin or 1 µg/ml puromycin plus 5 µg/ml Blasticidin S, which led to the substantial death of non-transfected cells over 4-6 days. Thereafter, selected cells were frozen in 10% DMSO and stored at -80°C. Expression was induced using 0.1 µg/ml doxycycline for 48 h. For S-CROSS, cells were grown for 2 days in selective medium, then 0.1 µg/ml doxycycline was applied and the cells were grown for additional 2 days before cross-linking experiments.

S-CROSS in cell extracts

At 48 h after protein expression induction, cells were lysed on 24 well plates (TPP) with Cellytic M (Sigma-Aldrich) supplemented with phosphatase (Sigma-Aldrich) and protease inhibitor cocktail (Sigma) in the presence of 3 µM cross-linker for 10 min at 37°C. Lysates were spun down for 20 min at +4°C at ~16000 g and supernatants were incubated additionally for 1 h at 37°C. Subsequently, samples were supplemented with SDS loading buffer and heated at 95°C for 5 min. Samples were then analyzed by SDS-PAGE and in-gel fluorescence scanning. The cross-linking score was determined using the following equation:

$$Score = \frac{2 * I_{crosslink} * 10^7}{\left(2 * I_{crosslink} + I_{partner\ A} + I_{partner\ B}\right) * I_{partner\ A} * I_{partner\ B}}$$

where $I_{cross\text{-}link}$ is the fluorescence intensity of the band corresponding to cross-linked proteins, $I_{partner\ A}$ and $I_{partner\ B}$ - the fluorescence intensities of the bands corresponding to labeled monomers. The term $I_{partner\ A} \times I_{partner\ B}$ is included in the denominator to correct for the interaction-independent crosslinking (i.e., background crosslinking). Scores were arbitrarily multiplied by a factor of 10^7.

SNAP-tag labeling and immunofluorescence

U2OS cells were grown on glass coverslips (0.17 µm thickness). Labeling of SNAP-constructs with cell permeable TMR-star or CP-Atto565 (0.3 µM, 1 h at 37˚C in DMEM + 10% FBS) was performed before fixation and pre-extraction. Prior to fixation, the culture medium was removed and cells were rapidly extracted with pre-warmed BRB80 buffer (37°C, 80 mM K-PIPES, pH 6.8, 1 mM $MgCl_2$; 1 mM EGTA, 0.2% NP-40) for 30 s. Subsequently, samples were fixed for 3-10 min in -20˚C methanol, washed in PBS and blocked for 60 min in 1% bovine serum albumin (BSA) in PBS. If labeling was not performed on live cells, SNAP-tagged proteins were labeled by incubating with 0.3 µM substrate (BG-547 or BG-Atto647N) in PBS containing 1% BSA for 1 h at room temperature. DNA was stained by ~0.1 µg/ml Hoechst 33342. Excess dye was then removed by washing 3 times with wash buffer (PBS containing 0.05% TX-100 reduced; Sigma-Aldrich). Labeling of live cells with CP-Atto565 permitted more sensitive detection of low levels of SNAP fusions on centrosome. Primary antibodies (listed below) were diluted in PBS with 1% BSA and added to the samples for overnight incubation at 4°C. Afterwards, the samples were washed 3 times and dilutions of secondary antibodies (listed

below) in PBS with 1% BSA were added for 1 h at room temperature. Samples for STED imaging were prepared in an identical manner except for omitting DNA staining with Hoechst 33342.

The following primary antibodies and dilutions were used: 1:2000 mouse anti-centrin [54] (clone 20H5; gift from Jeffrey Salisbury and currently available from Millipore), 1:400 mouse anti-C-Nap1 (BD Biosciences), 1:1000 mouse anti-HsSAS-6 and 1:500 rabbit anti-centrin 2 (both from Santa Cruz Biotechnology), 1:1000 rabbit anti-Cep57 (Abnova and Sigma-Aldrich), 1:2000 rabbit anti-STIL (Abcam), 1:1000 rabbit anti-Plk4 [55] (gift from Michel Bornens), 1:1000 rabbit anti-CPAP [9], mouse anti-FOP 1:1000 (clone 2B1, Abnova) 1:2000 rabbit anti-Cep63 (Millipore), 1:2000 rabbit anti-Cep152 (Sigma-Aldrich), 1:2000 mouse (clone GTU-88) and rabbit anti-γ-tubulin (Sigma-Aldrich).

The following secondary antibodies were used (all at 1:1000 – 1:500 dilution): goat anti-mouse or anti-rabbit coupled to Pacific blue (Invitrogen), Alexa 488 (Invitrogen), Alexa568 (Invitrogen), Alexa647 (Invitrogen), Chromeo494 (Active Motif) or Atto647N (Active Motif) and donkey anti-mouse or anti-rabbit coupled to Alexa568 (Invitrogen).

Direct labeling of rabbit anti-Cep57, anti-Cep63, anti-Cep152 and anti-Plk4 was performed using APEX™ Alexa Fluor® 488 or Alexa Fluor® 568 antibody labeling kits (Invitrogen) according to manufacturer protocols.

Confocal Microscopy, Image Processing, and Analysis

SNAP-tag and immunofluorescence labeled samples were imaged on a Zeiss LSM 710 (Zeiss, Germany) upright confocal microscope equipped with Plan-Apochromat 63x/1.40 Oil DIC M27 objective. Images were taken as z-stacks with voxel size 33 x 33 x 80 nm, pinhole 30 µm (0.5-0.6 AU) and averaging of 8. Images of TetraSpek fluorescent microspheres (200 nm, Invitrogen) were acquired before each imaging session. Color shift and PSF were calculated using Huygens Essentials (Scientific Volume Imaging). The acquired PSF (PSF distiller, Huygens Essentials package) was compared to the theoretical one. If no significant difference was observed, the theoretical PSF was used for deconvolution. Images were corrected for color shift (color shift corrector applet, Huygens Essentials package) before further processing. Subsequently, deconvolution was applied and colocalization of fluorescence signals was measured (Colocalization analyzer, Huygens Essentials package).

STED imaging was performed on a Leica TCS STED inverted system equipped with HCX PL APO 100x 1.40NA Oil objective. Images were taken as z-stacks with voxel size 20 x 20 x 126 nm, pinhole 1 AU and frame averaging of 8.

STED CW imaging was performed on a Leica TCS STED inverted system equipped with HCX PL APO 100.0x1.40 Oil objective. Images were taken as z-stacks with voxel size 20 x 20 x 126 nm, pinhole 0.25 AU and line averaging of 96. Resonance scanner was used for fast image acquisition to minimize sample drift effect. Images were presented as maximum intensity projections unless stated otherwise. Overlap of fluorescence signals was estimated using colocalization analyzer of Huygens Essentials package.

Protein expression in HEK293 cells

HEK293 cells were cultured in EX-CELL® 293 Serum-Free Medium (Sigma-Aldrich) in a humidified 5% CO_2 incubator at 37°C. Cells were split every 3-4 days or when reaching 2-3*10^6 cells/ml density. To generate inducible cell lines, cells were transiently transfected with pEBTet expression vector at 80-90% confluence. Cells (2 x 10^7) were collected and transfected in 1 ml RPMI1640 + 0.1% PLURONIC F-68 by adding 8 µg DNA and 25 µl polyethylenimine (stock 1 µg/µl) and incubating for 2h at 37°C. Afterwards, cells were diluted with 20 ml growth medium and incubated for 24 h in selective medium containing 3 µg/ml puromycin. At confluence, cells were split into 3 flasks containing 20 ml of medium each. The medium was replaced with selective medium containing 0.3 µg/ml doxycycline after reaching confluence. Cells were incubated for 48 h, collected, washed and frozen at -80°C until used for protein purification. An aliquot (2-5 ml) of cells was taken prior to protein expression induction in case if additional propagation would be needed.

Protein purification via FLAG-tag

Protein purification from frozen HEK293 cells was carried out using Sigma FLAG® M Purification Kit according to manufacturer recommendation. Protein elution from beads was achieved using 3xFLAG peptide. Finally, proteins were dialyzed against TBS (50 mM Tris-HCl pH 7.4, 150 mM NaCl, 2 mM 2-mercaptoethanol) containing 50% glycerol and stored at -20°C. Protein concentration was estimated using the Bradford method.

S-CROSS in vitro

200 - 300 nM proteins were mixed and incubated for 30 min at 37 ^oC in TBS (50 mM Tris-HCl pH 7.4, 150 mM NaCl, 2 mM 2-mercaptoethanol) containing 0.1 mg/ml BSA. The

BG-Cy5-BG homotypic cross-linker was added at 1 µM final concentration and the reaction mix was incubated for 1 h at 37 ^{o}C. The reaction was stopped by boiling the samples for 10 min at 95 ^{o}C in SDS-PAGE loading buffer. Afterwards, samples were analyzed by SDS-PAGE and in-gel fluorescence scanning.

RNA interference of Cep57, Cep63 and Cep152

Cep57, Cep63 and Cep152 were depleted using siRNAs listed in **Table S2**. Stealth RNAi siRNA negative control LO GC or Silencer® Select Negative Control No. 2 siLNA (Invitrogen) were used as controls. siRNA transfections were performed using Lipofectamine RNAiMax (Invitrogen) according to the manufacturer's protocol. Cells were analyzed after 72 h with the exception of cells treated with Cep57 siRNA B, which were analyzed after 48 h due to cell death at later time points. Cells treated with siRNAs were fixed following the procedure described above and stained with the following pairs of antibodies: anti-γ-tubulin and anti-Cep57, anti-γ-tubulin and anti-Cep63, anti-γ-tubulin and anti-Cep152 or anti-γ-tubulin and anti-centrin. After mounting samples in 90% glycerol (in PBS) containing 2.5% of n-propyl-gallate, cells were imaged on a Leica DMI6000B wide field microscope using a HCX PL APO 100x/1.47 Oil CORR oil immersion objective. Z-stacks were acquired in at least 16 regions using the tile scan function of coverslips. The resulting maximum intensity projections were processed with ImageJ and files analyzed with CellProfiler (version r10997), where the pipeline indentified the centrosomal region using the γ-tubulin signal and measured the maximal intensity in this region in the other channel. The calculated data were analyzed using GraphPad Prism 5 (Descriptive statistics).

The following siRNAs were used:

Cep57 A (siRNA, Microsynth)	CCATCAAGGTCTAATGGAAdTdT
Cep57 B (siRNA, Invitrogen)	UCGACGCUUGGAACUUGAGAGGAUU
Cep63 A (siRNA, Microsynth)	GGCUCUGGCUGAACAAUCAdTdT
Cep63 B (siLNA, Invitrogen)	GGAGCUCAUGAAACAGAUUTT
Cep152 A (siLNA, Invitrogen)	GGAUCCAACUGGAAAUCUATT
Cep152 B (siLNA, Invitrogen)	CUUUCGCGAUUCUAAUGAATT
STIL (siRNA, Invitrogen)	GAUAGGACUAAGUUCUCAUUGUUCA

Overexpression-induced co-localization at centrosomes

U2OS inducible cell lines expressing SNAP-constructs were cultured in 12-well glass-bottom dishes (Mattek) containing growth medium with 1 µg/ml puromycin and 0.3 µg/ml

doxycycline in a humidified 5% CO_2 incubator at 37˚C for 48 h. Labeling of SNAP-constructs was subsequently performed with TMR-star as described above. Labeled cells were fixed following the procedure described above and stained with the following pairs of antibodies: anti-centrin and anti-Cep57, anti-centrin and anti-Cep63, anti-centrin and anti-Cep152, anti-centrin and anti-FOP, or anti-centrin and anti-γ-tubulin. Finally, samples were cross-linked using 1 mM ethylene glycol bis(succinimidyl succinate) (EGS, Pierce). After brief washing with PBS, samples were stored in PBS containing ProClin 300 (Sigma-Aldrich) solution at 4˚C. Imaging and data processing in ImageJ were done as in the experiments with siRNA-treated samples. Files were analyzed with CellProfiler (version r10997), where the pipeline identified the centrosomal region using the centrin signal and measured the maximal intensity in this region in the two other channels. A threshold corresponding to 5-10% of maximal intensities measured in the SNAP-tag channel was applied to reduce the contribution of non-expressing cells. The calculated data were analyzed using GraphPad Prism 5 (Linear regression and Correlation).

FRET measurements

U2OS cells expressing the fusion proteins were labeled with CP-Atto565 (0.3 µM in DMEM + 10% FBS for 1 h at 37 ˚C). Afterwards, cells were fixed and stained with appropriate primary and secondary antibodies (labeled with either Alexa488 or Atto647N) as described above. FRET assays on fixed U2OS cells were performed using a Zeiss LSM 710 (Zeiss, Germany) upright confocal microscope equipped with Plan-Apochromat 63x/1.40 Oil DIC M27 objective. Images were taken with pixel size 33 x 33 nm, pinhole 1 AU and averaging of 8. Lasers used for reading were as follows: 488 nm set at 0.5 % power, 561 nm at 0.3 % and 633 nm at 0.5 %. Bleaching of Atto647N was performed by 700 scan iterations with 633 nm laser set to full power. The centrosome region and randomly chosen cytoplasmic regions were bleached. Intensity profiles in bleached regions were measured using Time Series Analyzer ImageJ plug-in. FRET efficiencies were calculated using the equation:

$$E = 1 - \frac{F_{pre-bleached}}{F_{post-bleached}}$$

where E: apparent FRET efficiency, $F_{\text{pre-bleached}}$: averaged (10 frames) donor (Atto565) fluorescence intensity before acceptor photobleaching and $F_{\text{post-bleached}}$: averaged (20 frames) donor (Atto565) fluorescence intensity after acceptor photobleaching.

Probing SNAP-STIL functionality

U2OS were maintained in McCoy's 5A GlutaMAX medium (Invitrogen) supplemented with 10% fetal bovine serum (FBS) tetracycline-negative (Brunschwig) for the inducible episomal cell lines. U2OS cell lines were generated using pEBTet-SNAP-GFP or pEBTet-SNAP-STIL plasmids as described above. Endogenous STIL was depleted using STIL siRNA targeting the 3′UTR. Stealth RNAi siRNA negative control LO GC (Invitrogen) was used as a control. siRNA transfection was performed using Lipofectamine RNAiMax (Invitrogen) according to the manufacturer's protocol, and cells were analyzed 48-72 hr after siRNA treatment.

U2OS cells grown on glass coverslips were fixed for 7–10 min in –20°C methanol, washed in PBS, and blocked in 1% bovine serum albumin and 0.05% Tween-20 in PBS. Cells were incubated for 2 h at room temperature with primary antibodies, washed three times for 10 min in PBST (0.05% Tween-20 in PBS), incubated 45 min at room temperature with secondary antibodies, stained with 1 µg/ml Hoechst 33258, washed three times in PBST, and mounted. Primary antibodies were 1:4000 mouse anti-centrin (20H5) and 1:2000 γ-Tubulin (Abcam). Secondary antibodies were 1:1000 goat anti-rabbit coupled to Alexa 488 and 1:1000 goat anti-mouse coupled to Alexa 568 (both from Invitrogen). For quantification of centrioles, mitotic cells were scored.

Synthesis of BG-Atto647N

All chemical reagents and dry solvents for synthesis were purchased from commercial suppliers (Sigma-Aldrich, Fluka, Acros, ATTO-TEC) and were used without further purification or distillation. The composition of mixed solvents is given by the volume ratio (v/v). Thin layer chromatography (TLC) was performed on TLC-aluminum sheets (Silica gel 60 F_{254}). Flash column chromatography was performed with Merck silica gel (230-400 mesh). ^{1}H and ^{13}C nuclear magnetic resonance (NMR) spectra were recorded on a Bruker DPX 400 (400 MHz for ^{1}H, 100 MHz for ^{13}C) or on a Bruker DRX-600 equipped with a cryoprobe, with chemical shifts (δ) reported in ppm relative to the solvent residual signals of DMSO-d_6 (2.50 ppm for ^{1}H, 39.52 ppm for ^{13}C) and coupling constants reported in Hz. High resolution mass spectra (HRMS) were measured on a Micromass Q-TOF Ultima spectrometer with electron spray ionization (ESI). Reversed phase analytical HPLC was run on a Waters 2790 separation module and products were detected at 280 nm using a

2487 dual λ absorption detector. The standard gradient that was used for the purifications started at water including 0.1% TFA for 2 minutes and increased to 100% acetonitrile within 17 minutes. A 3.9 × 300 mm Prep Nova-Pak HR C18 6 µm column from Waters was used to determine the purity of the products. Preparative HPLC was performed on a Waters 600 controller and with a Waters 2487 dual λ absorption detector using a SunFire™ Prep C18 OBD™ 5 µm 19 × 150 mm column.

The following abbreviations are used in the synthesis protocol: PyBOP: benzotriazole-1-yl-oxy-trispyrrolidinophosphonium hexafluorophosphate, DIEA: *N,N*-diisopropylethylamine, DMSO: dimethylsulfoxide, DMF: *N,N*-dimethylformamide, TFA: trifluoroacetic acid, TSTU: O-(N-Succinimidyl)-1,1,3,3-tetramethyluronium tetrafluoroborate. BG-NH_2 and CP-NH_2 were synthesized according to the previously reported literature [56, 57].

Fmoc-Lys(Me)$_3$-BG. Fmoc-Lys(Me)$_3$-OH hydrochloride (20.0 mg, 0.045 mmol, 1 eq.) and PyBOP (46.7 mg, 0.090 mmol, 2 eq.) were dissolved in DMSO (500 µl), and DIEA (25 µl, 0.1434 mmol, 3.2 eq.) was added to the reaction mixture and stirred at room temperature for 5 min. BG-NH_2 (20.5 mg, 0.076 mmol, 1.7 eq.) was then added to the reaction mixture and stirred further for 1 hr. The collected precipitates were subsequently dissolved in DMSO and purified by HPLC to afford white powder (27.7 mg, 80%).

^{1}H NMR (400 MHz, DMSO-d_6) δ 8.54 (t, 1 H, *J* = 5.8 Hz), 8.50 (s, 1 H), 7.90 (d, 2 H, *J* = 7.5 Hz), 7.74 (dd, 2 H, *J* = 7.3, 4.1 Hz), 7.63 (d, 1 H, *J* = 8.1 Hz), 7.49 (d, 2 H, *J* = 8.0 Hz), 7.42 (t, 2 H, *J* = 7.4 Hz), 7.32 (m, 4 H), 5.54 (s, 2 H), 4.29 (m, 5 H), 4.04 (m, 1 H), 3.26 (t, 2 H, *J* = 8.4 Hz), 3.04 (s, 9 H), 1.68 (m, 4 H), 1.31 (m, 2 H).

^{13}C NMR (100 MHz, DMSO-d_6) δ 172.3, 159.5, 158.9, 158.5, 156.5, 154.5, 144.4, 144.2, 141.2, 140.1, 134.8, 129.2, 128.1, 127.7, 127.5, 125.8, 120.6, 68.2, 66.1, 65.5, 55.0, 52.6, 47.2, 42.3, 31.8, 23.0, 22.2.

HRMS (ESI): *m/z* calc. for $C_{37}H_{43}N_8O_4$ 663.3407; found 663.3404 $[M]^+$ (-0.45 ppm)

BG-Atto647N. Fmoc-Lys(Me)$_3$-BG (3.0 mg, 3.86 µmol, 2 eq.) was dissolved in DMF (80 µl) and piperidine (20 µl) solution, and stirred at room temperature for 10 min. Et_2O/CH_2Cl_2 (1/1, v/v) solution was added to the reaction mixture and the precipitate was collected by centrifugation. The precipitate was washed with Et_2O/CH_2Cl_2 (1/1) to obtain H-Lys(Me)$_3$-BG as a white solid, which was used for the next reaction without further

purification. Atto-647N NHS ester (1.6 mg, 1.93 μmol, 1 eq.) was dissolved in DMSO (50 μl) and added to the solution of H-Lys(Me)$_3$-BG in DMSO (50 μl) in the presence of DIEA (2 μl), and stirred at room temperature for 2 hr. The reaction mixture was purified by HPLC and the resulting fraction was lyophilized to obtain BG-Atto647N as a blue powder (1.8 mg, 72%).

HRMS (ESI): *m/z* calc. for $C_{64}H_{83}N_{11}O_4$ 534.8315; found 534.8299 $[M/2]^+$ (-3.00 ppm). ATTO 647N is a cationic dye. After coupling of Atto647N-NHS to a substrate, the dye carries a net electrical charge of +1. (http://www.atto-tec.com/fileadmin/user_upload/Katalog_Flyer_Support/ATTO%20647N.pdf). Therefore, the net electrical charge of BG-Atto647N becomes +2.

Synthesis of CP-Atto565

To 60 μl of 10 mM solution of Atto565 6-isomer in DMSO (0.6 μmol, 1 eq.) were successively added 0.1 M TSTU in DMSO (8 μl, 0.8 μmol, 1.3 eq.) and DIEA (4 μl, 23 μmol, 38 eq.). After 1 min, 0.1 M CP-NH_2 in DMSO (10 μl, 1 μmol, 1.7 eq.) was added. The reaction was let 30 min at r.t., then 50 ul H_2O was added and the product was purified by HPLC and lyophilized to yield a pink powder (0.42 μmol, 70%).

^{1}H NMR (600 MHz, DMSO) δ 9.31 (t, 1 H, *J* = 5.9 Hz), 8.31 (d, 1 H, *J* = 8.2 Hz), 8.27 (dd, 1 H, *J* = 8.3, 1.6 Hz), 7.86 (d, 1 H, *J* = 1.4 Hz), 7.40 (d, 2 H, *J* = 8.1 Hz), 7.35 (d, 2 H, *J* = 8.1 Hz), 6.95 (s, 2 H), 6.70 (s, 2 H), 6.12 (s, 1 H), 5.29 (s, 2 H), 4.49 (d, 2 H, *J* = 5.4 Hz), 3.65 (q, 4 H, *J* = 6.8 Hz), 3.54 (m, 4 H), 2.65 (t, 4 H, *J* = 5.9 Hz), 1.84 (m, 4 H), 1.22 (t, 6 H, *J* = 7.1 Hz).

HRMS (ESI): *m/z* calc. for $C_{43}H_{42}N_6O_5Cl^+$ 757.2905; found 757.2916 $[M]^+$ (+1.45 ppm)

Supplemental References

1. Castiel, A., Danieli, M.M., David, A., Moshkovitz, S., Aplan, P.D., Kirsch, I.R., Brandeis, M., Kramer, A., and Izraeli, S. (2011). The Stil protein regulates centrosome integrity and mitosis through suppression of Chfr. J Cell Sci *124*, 532-539.
2. Kumar, A., Girimaji, S.C., Duvvari, M.R., and Blanton, S.H. (2009). Mutations in STIL, encoding a pericentriolar and centrosomal protein, cause primary microcephaly. Am J Hum Genet *84*, 286-290.
3. Stevens, N.R., Dobbelaere, J., Brunk, K., Franz, A., and Raff, J.W. (2010). Drosophila Ana2 is a conserved centriole duplication factor. J Cell Biol *188*, 313-323.
4. Vulprecht, J., David, A., Tibelius, A., Castiel, A., Konotop, G., Liu, F., Bestvater, F., Raab, M.S., Zentgraf, H., Izraeli, S., et al. (2012). STIL is required for centriole duplication in human cells. J Cell Sci *125*, 1353-1362.
5. Sonnen, K.F., Schermelleh, L., Leonhardt, H., and Nigg, E.A. (2012). 3D-structured illumination microscopy provides novel insight into architecture of human centrosomes. Biol Open *1*, 965-976.
6. Tang, C.J., Lin, S.Y., Hsu, W.B., Lin, Y.N., Wu, C.T., Lin, Y.C., Chang, C.W., Wu, K.S., and Tang, T.K. (2011). The human microcephaly protein STIL interacts with CPAP and is required for procentriole formation. EMBO J *30*, 4790-4804.
7. Kitagawa, D., Kohlmaier, G., Keller, D., Strnad, P., Balestra, F.R., Fluckiger, I., and Gönczy, P. (2011). Spindle positioning in human cells relies on proper centriole formation and on the microcephaly proteins CPAP and STIL. J Cell Sci *124*, 3884-3893.
8. Strnad, P., Leidel, S., Vinogradova, T., Euteneuer, U., Khodjakov, A., and Gönczy, P. (2007). Regulated HsSAS-6 levels ensure formation of a single procentriole per centriole during the centrosome duplication cycle. Dev Cell *13*, 203-213.
9. Kohlmaier, G., Loncarek, J., Meng, X., McEwen, B.F., Mogensen, M.M., Spektor, A., Dynlacht, B.D., Khodjakov, A., and Gönczy, P. (2009). Overly long centrioles and defective cell division upon excess of the SAS-4-related protein CPAP. Curr Biol *19*, 1012-1018.
10. Brown, N., and Costanzo, V. (2009). An ATM and ATR dependent pathway targeting centrosome dependent spindle assembly. Cell Cycle *8*, 1997-2001.
11. Loffler, H., Fechter, A., Matuszewska, M., Saffrich, R., Mistrik, M., Marhold, J., Hornung, C., Westermann, F., Bartek, J., and Kramer, A. (2011). Cep63 recruits Cdk1 to the centrosome: implications for regulation of mitotic entry, centrosome amplification, and genome maintenance. Cancer Res *71*, 2129-2139.
12. Smith, E., Dejsuphong, D., Balestrini, A., Hampel, M., Lenz, C., Takeda, S., Vindigni, A., and Costanzo, V. (2009). An ATM- and ATR-dependent checkpoint inactivates spindle assembly by targeting CEP63. Nat Cell Biol *11*, 278-285.
13. Momotani, K., Khromov, A.S., Miyake, T., Stukenberg, P.T., and Somlyo, A.V. (2008). Cep57, a multidomain protein with unique microtubule and centrosomal localization domains. Biochem J *412*, 265-273.
14. Ruiz-Miro, M., Colomina, N., Fernandez, R.M., Gari, E., Gallego, C., and Aldea, M. (2011). Translokin (Cep57) interacts with cyclin D1 and prevents its nuclear accumulation in quiescent fibroblasts. Traffic *12*, 549-562.
15. Snape, K., Hanks, S., Ruark, E., Barros-Nunez, P., Elliott, A., Murray, A., Lane, A.H., Shannon, N., Callier, P., Chitayat, D., et al. (2011). Mutations in CEP57 cause mosaic variegated aneuploidy syndrome. Nat Genet *43*, 527-529.
16. Shi, X., Sun, X., Liu, M., Li, D., Aneja, R., and Zhou, J. (2011). CEP70 Protein Interacts with {gamma}-Tubulin to Localize at the Centrosome and Is Critical for Mitotic Spindle Assembly. J Biol Chem *286*, 33401-33408.
17. Wilkinson, C.J., Carl, M., and Harris, W.A. (2009). Cep70 and Cep131 contribute to ciliogenesis in zebrafish embryos. BMC Cell Biol *10*, 17.

18. Cizmecioglu, O., Arnold, M., Bahtz, R., Settele, F., Ehret, L., Haselmann-Weiss, U., Antony, C., and Hoffmann, I. (2010). Cep152 acts as a scaffold for recruitment of Plk4 and CPAP to the centrosome. J Cell Biol *191*, 731-739.
19. Dzhindzhev, N.S., Yu, Q.D., Weiskopf, K., Tzolovsky, G., Cunha-Ferreira, I., Riparbelli, M., Rodrigues-Martins, A., Bettencourt-Dias, M., Callaini, G., and Glover, D.M. (2010). Asterless is a scaffold for the onset of centriole assembly. Nature *467*, 714-718.
20. Hatch, E.M., Kulukian, A., Holland, A.J., Cleveland, D.W., and Stearns, T. (2010). Cep152 interacts with Plk4 and is required for centriole duplication. J Cell Biol *191*, 721-729.
21. Paoletti, A., Moudjou, M., Paintrand, M., Salisbury, J.L., and Bornens, M. (1996). Most of centrin in animal cells is not centrosome-associated and centrosomal centrin is confined to the distal lumen of centrioles. J Cell Sci *109 (Pt 13)*, 3089-3102.
22. Knorz, V.J., Spalluto, C., Lessard, M., Purvis, T.L., Adigun, F.F., Collin, G.B., Hanley, N.A., Wilson, D.I., and Hearn, T. (2010). Centriolar association of ALMS1 and likely centrosomal functions of the ALMS motif-containing proteins C10orf90 and KIAA1731. Mol Biol Cell *21*, 3617-3629.
23. Kenedy, A.A., Cohen, K.J., Loveys, D.A., Kato, G.J., and Dang, C.V. (2003). Identification and characterization of the novel centrosome-associated protein CCCAP. Gene *303*, 35-46.
24. Otto, E.A., Hurd, T.W., Airik, R., Chaki, M., Zhou, W., Stoetzel, C., Patil, S.B., Levy, S., Ghosh, A.K., Murga-Zamalloa, C.A., et al. (2010). Candidate exome capture identifies mutation of SDCCAG8 as the cause of a retinal-renal ciliopathy. Nat Genet *42*, 840-850.
25. Andersen, J.S., Wilkinson, C.J., Mayor, T., Mortensen, P., Nigg, E.A., and Mann, M. (2003). Proteomic characterization of the human centrosome by protein correlation profiling. Nature *426*, 570-574.
26. Acquaviva, C., Chevrier, V., Chauvin, J.P., Fournier, G., Birnbaum, D., and Rosnet, O. (2009). The centrosomal FOP protein is required for cell cycle progression and survival. Cell Cycle *8*, 1217-1227.
27. Mikolajka, A., Yan, X., Popowicz, G.M., Smialowski, P., Nigg, E.A., and Holak, T.A. (2006). Structure of the N-terminal domain of the FOP (FGFR1OP) protein and implications for its dimerization and centrosomal localization. J Mol Biol *359*, 863-875.
28. Bettencourt-Dias, M., and Carvalho-Santos, Z. (2008). Double life of centrioles: CP110 in the spotlight. Trends Cell Biol *18*, 8-11.
29. Chen, Z., Indjeian, V.B., McManus, M., Wang, L., and Dynlacht, B.D. (2002). CP110, a cell cycle-dependent CDK substrate, regulates centrosome duplication in human cells. Dev Cell *3*, 339-350.
30. Spektor, A., Tsang, W.Y., Khoo, D., and Dynlacht, B.D. (2007). Cep97 and CP110 suppress a cilia assembly program. Cell *130*, 678-690.
31. Tsang, W.Y., Bossard, C., Khanna, H., Peranen, J., Swaroop, A., Malhotra, V., and Dynlacht, B.D. (2008). CP110 suppresses primary cilia formation through its interaction with CEP290, a protein deficient in human ciliary disease. Dev Cell *15*, 187-197.
32. Tsang, W.Y., Spektor, A., Vijayakumar, S., Bista, B.R., Li, J., Sanchez, I., Duensing, S., and Dynlacht, B.D. (2009). Cep76, a centrosomal protein that specifically restrains centriole reduplication. Dev Cell *16*, 649-660.
33. Jeffery, J.M., Urquhart, A.J., Subramaniam, V.N., Parton, R.G., and Khanna, K.K. (2010). Centrobin regulates the assembly of functional mitotic spindles. Oncogene.
34. Zou, C., Li, J., Bai, Y., Gunning, W.T., Wazer, D.E., Band, V., and Gao, Q. (2005). Centrobin: a novel daughter centriole-associated protein that is required for centriole duplication. J Cell Biol *171*, 437-445.
35. Gache, V., Waridel, P., Winter, C., Juhem, A., Schroeder, M., Shevchenko, A., and Popov, A.V. (2010). Xenopus meiotic microtubule-associated interactome. PLoS One *5*, e9248.
36. Graser, S., Stierhof, Y.D., Lavoie, S.B., Gassner, O.S., Lamla, S., Le Clech, M., and Nigg, E.A. (2007). Cep164, a novel centriole appendage protein required for primary cilium formation. J Cell Biol *179*, 321-330.

37. Guderian, G., Westendorf, J., Uldschmid, A., and Nigg, E.A. (2010). Plk4 trans-autophosphorylation regulates centriole number by controlling betaTrCP-mediated degradation. J Cell Sci *123*, 2163-2169.
38. Kleylein-Sohn, J., Westendorf, J., Le Clech, M., Habedanck, R., Stierhof, Y.D., and Nigg, E.A. (2007). Plk4-induced centriole biogenesis in human cells. Dev Cell *13*, 190-202.
39. Tang, C.J., Fu, R.H., Wu, K.S., Hsu, W.B., and Tang, T.K. (2009). CPAP is a cell-cycle regulated protein that controls centriole length. Nat Cell Biol *11*, 825-831.
40. Zhao, L., Jin, C., Chu, Y., Varghese, C., Hua, S., Yan, F., Miao, Y., Liu, J., Mann, D., Ding, X., et al. (2010). Dimerization of CPAP orchestrates centrosome cohesion plasticity. J Biol Chem *285*, 2488-2497.
41. Azimzadeh, J., Hergert, P., Delouvee, A., Euteneuer, U., Formstecher, E., Khodjakov, A., and Bornens, M. (2009). hPOC5 is a centrin-binding protein required for assembly of full-length centrioles. J Cell Biol *185*, 101-114.
42. Martinez-Sanz, J., Yang, A., Blouquit, Y., Duchambon, P., Assairi, L., and Craescu, C.T. (2006). Binding of human centrin 2 to the centrosomal protein hSfi1. FEBS J *273*, 4504-4515.
43. Oshimori, N., Li, X., Ohsugi, M., and Yamamoto, T. (2009). Cep72 regulates the localization of key centrosomal proteins and proper bipolar spindle formation. EMBO J *28*, 2066-2076.
44. Coppieters, F., Lefever, S., Leroy, B.P., and De Baere, E. (2010). CEP290, a gene with many faces: mutation overview and presentation of CEP290base. Hum Mutat *31*, 1097-1108.
45. Gautier, A., Nakata, E., Lukinavicius, G., Tan, K.T., and Johnsson, K. (2009). Selective cross-linking of interacting proteins using self-labeling tags. J Am Chem Soc *131*, 17954-17962.
46. Jiang, K., and Akhmanova, A. (2011). Microtubule tip-interacting proteins: a view from both ends. Curr Opin Cell Biol *23*, 94-101.
47. Raynaud-Messina, B., and Merdes, A. (2007). Gamma-tubulin complexes and microtubule organization. Curr Opin Cell Biol *19*, 24-30.
48. Kitagawa, D., Vakonakis, I., Olieric, N., Hilbert, M., Keller, D., Olieric, V., Bortfeld, M., Erat, M.C., Fluckiger, I., Gönczy, P., et al. (2011). Structural basis of the 9-fold symmetry of centrioles. Cell *144*, 364-375.
49. Coppieters, F., Casteels, I., Meire, F., De Jaegere, S., Hooghe, S., van Regemorter, N., Van Esch, H., Matuleviciene, A., Nunes, L., Meersschaut, V., et al. (2010). Genetic screening of LCA in Belgium: predominance of CEP290 and identification of potential modifier alleles in AHI1 of CEP290-related phenotypes. Hum Mutat *31*, E1709-1766.
50. Kollman, J.M., Polka, J.K., Zelter, A., Davis, T.N., and Agard, D.A. (2010). Microtubule nucleating gamma-TuSC assembles structures with 13-fold microtubule-like symmetry. Nature *466*, 879-882.
51. Durussel, I., Blouquit, Y., Middendorp, S., Craescu, C.T., and Cox, J.A. (2000). Cation- and peptide-binding properties of human centrin 2. FEBS Lett *472*, 208-212.
52. Bach, M., Grigat, S., Pawlik, B., Fork, C., Utermohlen, O., Pal, S., Banczyk, D., Lazar, A., Schomig, E., and Grundemann, D. (2007). Fast set-up of doxycycline-inducible protein expression in human cell lines with a single plasmid based on Epstein-Barr virus replication and the simple tetracycline repressor. FEBS J *274*, 783-790.
53. Purvis, T.L., Hearn, T., Spalluto, C., Knorz, V.J., Hanley, K.P., Sanchez-Elsner, T., Hanley, N.A., and Wilson, D.I. (2010). Transcriptional regulation of the Alstrom syndrome gene ALMS1 by members of the RFX family and Sp1. Gene *460*, 20-29.
54. Sanders, M.A., and Salisbury, J.L. (1994). Centrin plays an essential role in microtubule severing during flagellar excision in Chlamydomonas reinhardtii. J Cell Biol *124*, 795-805.
55. Sillibourne, J.E., Tack, F., Vloemans, N., Boeckx, A., Thambirajah, S., Bonnet, P., Ramaekers, F.C., Bornens, M., and Grand-Perret, T. (2010). Autophosphorylation of polo-like kinase 4 and its role in centriole duplication. Mol Biol Cell *21*, 547-561.
56. Keppler, A., Gendreizig, S., Gronemeyer, T., Pick, H., Vogel, H., and Johnsson, K. (2003). A general method for the covalent labeling of fusion proteins with small molecules in vivo. Nat Biotechnol *21*, 86-89.

57. Srikun, D., Albers, A.E., Nam, C.I., Iavarone, A.T., and Chang, C.J. (2010). Organelle-targetable fluorescent probes for imaging hydrogen peroxide in living cells via SNAP-Tag protein labeling. J Am Chem Soc *132*, 4455-4465.